

DISSOLUTION RATE OF SPECIFIC ELEMENTS IN SAC305 SOLDER

David Hillman, Ross Wilcoxon, Tim Pearson, Paul McKenna
Rockwell Collins
IA, USA
david.hillman@rockwellcollins.com

ABSTRACT

The 2005 Restriction of Hazardous Substances (RoHS) European Union Directive has significantly reduced the use of tin/lead surface finishes for component terminations. A reexamination of solder joint wetting of lead-free solders with the new component terminations is key to establishing thermal process profiles that ensure acceptable solder joint integrity. One example of how the interactions between solder and surface finish can affect solder joint integrity is the potential formation of brittle gold/tin intermetallic compounds (IMCs) when the solder gold content exceeds 5% by weight. Controlling the component gold plating thickness as well as the soldering process temperature and time can prevent gold embrittlement. For decades, the electronics industry has relied on the results published by W.G. Bader in 1969 to relate process temperature and time to surface finish dissolution rates in defining acceptable soldering process profiles for tin/lead surface finishes. Because comparable data for lead-free solders are not available, testing was conducted to update Bader's results to address the needs for today's lead-free soldering applications. A series of soldering dissolution experiments, modeled on Bader's, were conducted using SAC305 solder with gold, silver, palladium, platinum, copper and nickel samples. This paper describes the test approach for measuring the solder dissolution of these materials and reports dissolution rates that can be used to optimize soldering process profiles for electronic assemblies.

Key words: Dissolution rates, SAC305 Solder

BACKGROUND

The proper metallurgical combination of the component surface finish, the printed circuit board finish and the solder alloy is critical in forming reliable solder joints. Since a metallurgically sound connection requires that the solder alloy be compatible with the surface finishes, producing reliable solder joints relies on intimate knowledge of how the solder and surface finishes react for specific temperature/time profiles. In 1969, W. G. Bader conducted an experiment to determine the dissolution rates of various elements in a Sn60Pb40 eutectic solder alloy [1]. Bader's

testing included gold (Au), silver (Ag), copper (Cu), nickel (Ni), palladium (Pd) and platinum (Pt), which were the industry's primary surface finishes for components and printed circuit boards. The dissolution rates measured by Bader have been used by the electronics industry for 50 years to establish acceptable soldering profiles and reliable solder joints. The introduction of the 2005 Restriction of Hazardous Substances (RoHS) European Union Directive accelerated the replacement of tin/lead solders with lead-free solder alloys such as Sn3.0Ag0.5Cu (SAC305) solder. Lead-free solder alloys generally have higher melting temperatures that alter solder processing profiles (temperature as well as time). The application of RoHS also reduced the use of tin/lead surface finishes, leading to a resurgence of the use of Au, Ag, and Pd as primary component surface finishes and a reemergence of detrimental solder joint metallurgical phenomena associated with these materials.

Gold plating has been widely used as both a component and a board surface finish, due to its resistance to the formation of an oxide layer that prevents solder wetting. However, gold has two primary disadvantages; (1) the cost of gold is relatively high, as compared to other surface finishes; (2) gold and tin can form a brittle intermetallic compound (IMC). The formation of the AuSn₄ IMC needle-like structure occurs when the gold content of a solder joint exceeds 3-5 percent by weight (%w) and significantly degrades the solder joint integrity [2 - 5]. Figure 1 illustrates both optical and scanning electron microscopy (SEM) images of the brittle AuSn₄ IMC.



Figure 1: Gold-Tin IMC Images- Optical (left), SEM (right)

Gold surface finishes have been successfully utilized in the electronics industry through precise control of solder time, temperature and solder volume to avoid the formation of detrimental metallurgical phases. Numerous published investigations have described how to avoid gold embrittlement issues in solder joints (Puttlitz and Stalter [6], Kein Wassink [7], Lea [8]).

The use of silver as a component surface finish has traditionally been to limited ceramic bodied components, such as leadless ceramic chip carriers (LCCCs) or light emitting diodes (LEDs), in which silver is a constituent of the metal-glass fired ink termination. The electronics industry has widely used immersion silver surface finishes for printed circuit boards with silver plating thickness of 0.13-0.41 micron (5-16 microinches). The primary silver IMC formed in solder joints is Ag_3Sn , they occupy only very small portions of the solder joint microstructure and are not considered a solder joint integrity degradation root cause. Excessive Ag_3Sn IMCs resulting from improper soldering processes, as shown in Figure 2, have the potential for causing solder joint integrity issues but are rarely attributed as being a solder joint failure root cause [9, 10]. Wilcoxon et al. demonstrated that immersion silver surface finishes with plating thicknesses in the 0.38-0.76 micron (15-30 microinches) produced solder joints with an acceptably small level of degradation after 2000 thermals cycles between -55°C to +125°C [11].

The solder joint degradation that was observed was due to the impact of the silver on the bulk properties of the solder, rather than the formation of a distinct detrimental silver/tin IMC phase.

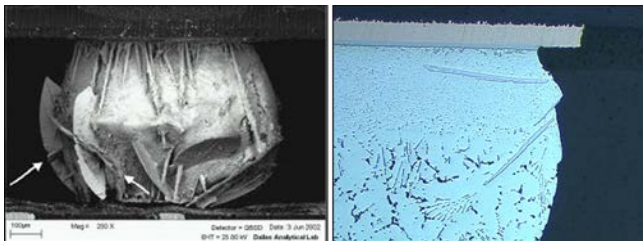


Figure 2: Excessively Large Ag_3Sn IMC Plates in BGA Solder Joints (left: [9], right: [10])

Palladium has seen a resurgence in use as a surface finish with the increasing application of lead-free soldering technology. Prior to RoHS, palladium was primarily found in ceramic bodied components as a constituent of the metal-glass fired ink termination in combination with platinum or silver (i.e. Pt/Pd/Ag or Pd/Ag). Texas Instruments introduced the use of palladium as part of the Ni/Pd/Au component surface finish for plastic packaged integrated

circuits (ICs) in 1989 as part of an effort to eliminate lead from their component fabrication processes [12,13]. Vianco et al. [14] investigated the impact of palladium on solder joint integrity by looking at mechanical/thermal cycling and metallurgical reactions. They found that the palladium behaved much like gold in forming a brittle IMC, $PdSn_4$, but with a lower solder joint concentration limit range of 1-2%w. The investigation concluded that nickel/palladium was a viable surface finish but, with its slow dissolution rate, as documented by Bader [1], the significant potential of palladium embrittlement drives a need for very tight soldering process time/temperature controls. Other published research results have been in general agreement with the Vianco investigation (Pratt [15], Wolverton [16], Tegehall [17], and Chen [18]). The printed circuit board community has significant interest in the use of palladium since electroless nickel (EN)/electroless palladium (EP)/immersion gold (IG) (ENEPIG) has become more widely used, due to its solderability and wirebondability characteristics. Industry investigations (Mei and Eslambolchi [19], Gumpert [20], Wolverton [21]) have demonstrated the same potential palladium embrittlement issues with printed circuit board finishes if the soldering process is not adequately controlled. Figure 3 illustrates the $PdSn_4$ IMC phase in a solder joint/nickel plating printed circuit board interface for both tin/lead and lead-free solder processes.

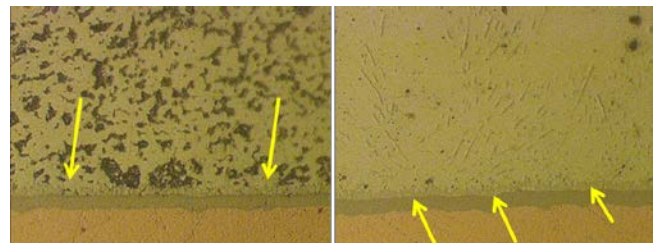


Figure 3: $PdSn_4$ IMC Structure in Solder Joints, Tin/lead (left), SAC305 (right)

Currently, the use of platinum as a surface finish is fairly rare in component construction. Platinum, in combination with palladium or silver (i.e. Pt/Pd/Ag or Pt/Ag), is primarily found on ceramic bodied components as constituent of the metal-glass fired ink termination. Platinum is also used in some microelectronic hybrid circuits as it is both wire bondable and solderable, due to its oxide-resistant characteristics.

Since soldering to copper and nickel interfaces is a fundamental practice for the electronics industry, understanding the dissolution rate of these elements is essential to prevent excessive copper removal, particularly in rework activities. The dissolution rate of nickel in tin/lead

solder is significantly lower than that of copper; some electronic designs take advantage of that to improve their soldering process robustness. Figure 4 illustrates how nickel plating eliminated the risk of damage to plated through-hole knees due to copper dissolution.

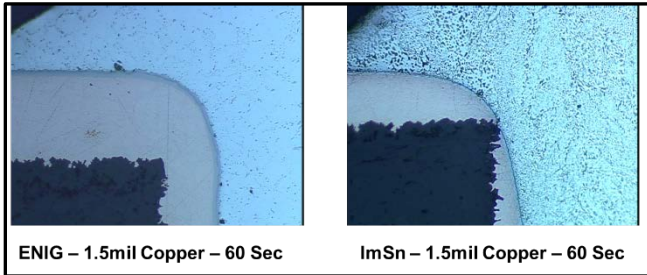


Figure 4: Impact of Nickel Plating Versus Soldering Process Dissolution Rates: ENIG PTH (left), Immersion Tin (ImSn) PTH (right)

However, nickel plating/interfaces have their own set of problems, with brittle nickel fracture being the most significant. Tin/lead solder alloys form two primary IMCs with copper (Cu_6Sn_5 and Cu_3Sn) to create an elastic interface with tin/lead solder. Tin/lead soldering to nickel produces either Ni_3Sn_4 or $(\text{Cu}, \text{Ni})_6\text{Sn}_5$, which have a less elastic interface [17]. With an elastic modulus that is 33% higher than tin/lead, SAC305 for example, induces higher stresses that lead to brittle nickel fracture that can be more likely in lead free solder joints than in tin/lead solder joints [22].

Because of the relatively low dissolution rate of copper in the eutectic tin/lead solder, copper dissolution was historically not a major issue under typical soldering durations and temperatures. However, the use of lead-free solders led to major soldering process changes as the electronics industry addressed the much higher copper dissolution rates associated with lead-free solders and their reflow temperatures. With knowledge of the dissolution rate of copper for a specific lead-free solder alloy, the process engineer can establish the “edge of the cliff” with regards to excessive copper removal. As an example, Figure 5 illustrates how the lower copper dissolution rate for the SN100C lead-free solder alloy allows for a longer soldering duration window than the higher dissolution rate SAC305 lead-free solder alloy [23].

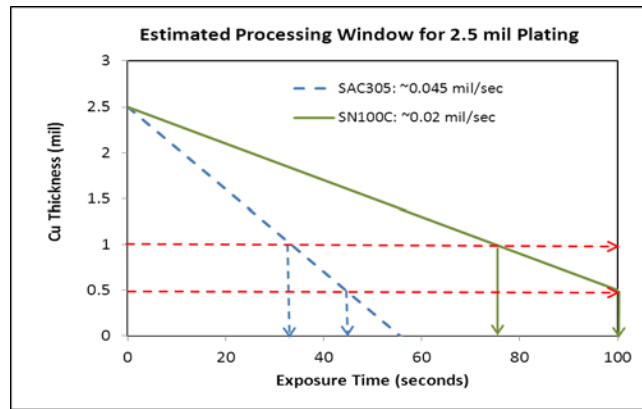


Figure 5: The Impact of SN100C Versus SAC305 Lead-free Solder Alloys on Copper Thickness Based on Alloy Copper Dissolution Rates

Understanding the dissolution rates of specific elements in a SAC305 solder alloy provides the data necessary to define appropriate solder process temperatures and dwell times for creating consistent solder joints. Bader’s calculated element dissolution rates have been critical in creating acceptable tin/lead soldering process parameters that lead to reliable solder joints. Comparable data sets for the lead-free solder alloy are necessary to allow process engineers to meet the needs of today’s electronics assembly processes.

INVESTIGATION PARAMETERS

Elements

The six elements selected for the investigation were gold (Au), silver (Ag), palladium (Pd), platinum (Pt), copper (Cu), and nickel (Ni). These elements were the same elements investigated by Bader and five of them represent the most common elements currently used in the electronics industry for plating and surface finishes. While platinum has only a minor presence as a surface finish, it was included in part to mimic the Bader study but also because its dissolution rate was of a material science interest to the authors.

Solder Alloy

SAC305 (96.5% tin, 3% silver, and 0.5% copper) is the most widely used lead-free solder alloy in the electronics industry. Extensive reliability and manufacturability studies have led to the alloy seeing growing use in some high performance, high reliability product use environments. The SAC305 solder alloy is one of three approved lead-free solder alloys for Rockwell Collins production use.

Temperature and Dwell Time

A wide range of temperatures and dwell times were selected to create a data set that would allow for an accurate determination of the dissolution rates of the selected

elements. The maximum temperature/dwell time parameters were partially dictated by each specific element. For example, the testing of gold at 260°C was limited to a 20 second maximum dwell, since longer dwell times resulted in the complete dissolution of the test sample. Table 1 summarizes the times and temperatures used for each material included in the study.

Table 1: Investigation Temperatures and Immersion Times

	Temp. (°C)	Time (sec)		Temp. (°C)	Time (sec)
Au	220	10, 20, 40, 60	Pd	240	10, 20, 40, 60, 80, 120
	230	10, 20, 40		290	
	240	10, 20		340	
	250			390	
	260			440	
Ag	230	10, 20, 40, 60, 80, 120	Cu	250	10, 20, 40, 60, 80, 120
	250			275	
	260	10, 20, 40, 60, 80		300	
	270			325	
	290			350	
Pt	310	10, 20, 40	400	10, 20, 40	
	330	10, 20, 40, 60, 80, 120	450	10, 20	
	360		Ni	330	10, 20, 40, 60, 80, 120
	390	360			
	420	390			
450	420				
				450	

OBJECTIVE

The objective of the investigation was to determine the dissolution rates for gold (Au), silver (Ag), palladium (Pd), platinum (Pt), copper (Cu) and nickel (Ni) in a SAC305 solder alloy.

PROCEDURES

Test Wires

Test wires were procured from Goodfellow and Materion in a spool format. A total of three test wires were processed for each time/temperature combination. Table 2 lists the wire purity and diameter, with tolerance, specified by the supplier. For reference, Table 2 shows the diameters in metric and US customary units with values in parenthesis indicating the equivalent value to the dimension reported by the supplier.

Table 2: Test Wire Details

Element	Purity	Wire Diameter	
		mm	mil
Cu	99.90%	0.5 ± 0.05	(19.7 ± 1.97)
Ni	99.90%	0.5 ± 0.05	(19.7 ± 1.97)
Ag	99.00%	(0.508 ± 0.0127)	20 ± 0.5
Au	99.99%	(0.508 ± 0.0127)	20 ± 0.5
Pt	99.99%	(0.508 ± 0.0127)	20 ± 0.5

Pd	99.95%	(0.508 ± 0.0076)	20 ± 0.3
----	--------	------------------	----------

Wire samples were unwound from the manufacturer spool and cut into 1.5 inch lengths. Care was taken to ensure that the diameter of the wire sample at the area of interest was not deformed in the cutting process. The wire test fixture consisted of an adhesive dispensing syringe tip with a 22 gauge contact connector attached to the end of the syringe needle. This arrangement securely held the test wires without inducing deformation. The syringe needle was taped to a flat rectangular sheet of aluminum attached to the test dipping apparatus. This wire test fixture kept the test wires perpendicular to the surface of the solder bath and allowed for easy/safe handling of the wires after fluxing and after immersion in the solder bath (Figure 6).



Figure 6: Wire Test Fixture (left), Fixture Installed on Test Dipping Apparatus (right)

Test Dipping Apparatus

The test dipping apparatus consisted of two main parts: the Velmex stepper motor assembly/controller and the wire test fixture. The dipping apparatus, shown in Figure 7, consisted of a two phase stepping motor that rotated a long carrier screw to vertically move a boom arm that held the wire test fixture. The Velmex controller was operated using simple loop codes that allowed for very precise, repeatable and controlled dipping speed, depth, and immersion time that a given sample spent in the solder bath. The solder bath held approximately 900g of solder. This quantity of solder was assumed to be large enough that dissolution of materials during the testing of a set of samples would not sufficiently alter the composition of the solder such that its properties would change.

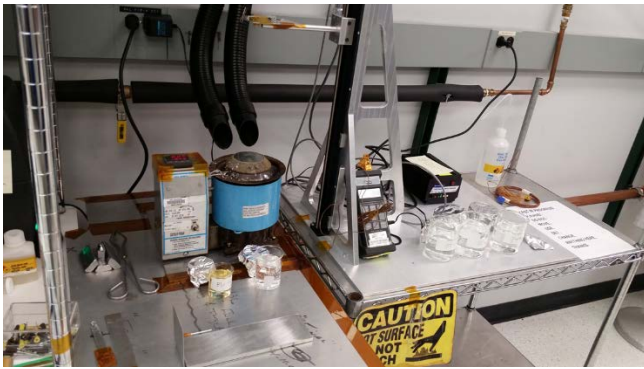


Figure 7: Test Dipping Apparatus and Test Setup

Test Procedure

The following test procedure for dipping the test wires was used:

1. Adjust solder pot to specified test temperature and verify using independent thermocouple.
 - a. Remove solder pot sample and label as initial element test solder pot composition.
2. Insert test wire into wire test fixture.
3. Dip test wire in Blackstone 1452 soldering flux to a dip depth of 2.54 cm (1 inch) for 5-10 seconds, remove from flux and attach to test dipping apparatus. Note: an acid flux was used to minimize potential wetting induced variation.
4. Skim solder dross from solder pot.
5. Initiate solder dipping program, dipping test wire to 2.54 cm (1 inch) depth for the specified time interval.
6. After removal from the solder bath, immediately quench test wire in deionized water. The time interval between removal from the solder bath and quenching to be in the range of 0.3 -1.0 seconds.
 - a. Remove test wire from wire test fixture and remove flux residues.
7. Solder pot was thoroughly stirred after each specific temperature interval.
8. Repeat process for the entire specified element time/temperature interval set.
9. Replace solder bath with virgin SAC305 solder for next specified element.
 - a. Remove solder pot sample and label for final element test solder pot composition assessment.

Post Solder Dipping Test Wire Processing

The cleaned test wires were metallographically cross-sectioned, transverse to the wire axis, at a distance of 0.635 cm (0.25 inches) from the dipped end to expose the test wire diameter-solder interface. The reduced test wire area due to dissolution was calculated using the “Measure polyline or polyline” tool in the Clemex Vision Lite software on an Olympus BH-2 microscope at a nominal magnification of 100X. Once samples were magnified, the “measure polyline or polygon tool” was used to precisely trace a path around

the perimeter of the solder alloy sample. This calculated the exact area within the path regardless of the shape the sample had taken after dissolution in the solder bath. The cross sectional area was determined three times for each sample by drawing three separate paths on the sample and the three measurements were then averaged. This was done to improve the measurement consistency by reducing the effects of how the operator selected points to define the solder boundary. Figure 8 illustrates a finished cross-section and measured test wire sample.

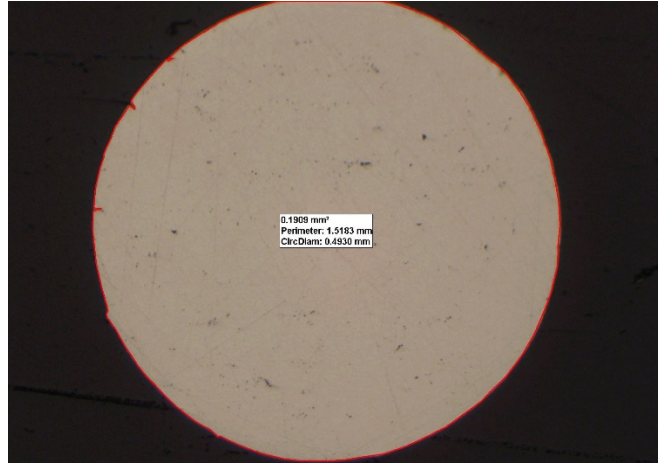


Figure 8: Measured Test Wire Sample (Silver, 250°C, 10 seconds)

DISSOLUTION RATE & ARRHENIUS COEFFICIENT DETERMINATIONS

The area measured with the optical inspection method (A_{meas}) was used to determine an effective radius, r , of the sample by assuming that the wire maintained a circular cross section, so that $A_{meas} = \pi r^2$. Thus, the effective radius was calculated as $r = \sqrt{A_{meas} / \pi}$. The wire radius was plotted as a function of immersion time for each solder bath temperature used for a given material. Figure 9a shows an example of this data for the gold wire in SAC305; symbols indicate the radii as calculated from the cross sectional area while lines indicate linear curve fits.

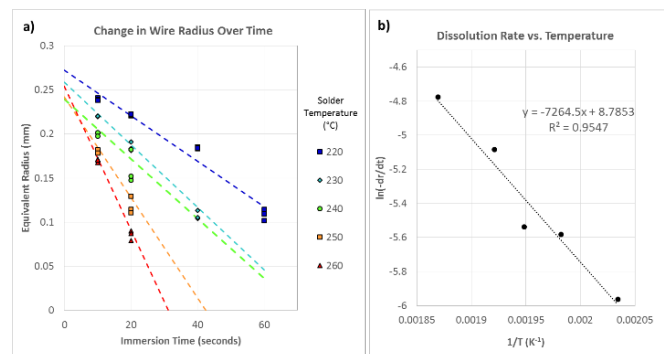


Figure 9: Example of Dissolution Data for Gold in SAC305 Solder

The dissolution rates for the material were determined for each solder bath temperature as the negative of slope of the line $(-dr/dt)$ for the data set for each bath temperature. The curve fits for each data set used to determine the dissolution rate, along with the raw data, are shown in Figure 9a. Note that the reported diameter of the gold wire was 20 ± 0.5 mil (0.508 ± 0.0127 mm). Thus, the initial radius of the wire should be within the range of 0.248 – 0.260mm. The intercept value for each data set (radius for an immersion time of 0 seconds) falls within that range, but is not precisely the same for each set. This indicates that initial radius of each sample was, in fact, not likely to be exactly the same.

To compare the data to each other and to past studies, the temperature dependence of the dissolution rate was assumed to follow the Arrhenius equation, shown in Equation {1}:

$$\frac{dr}{dt} = Ae^{\frac{-E}{RT}}$$

where A is a constant, E is the activation energy, R is the universal gas constant, and T is the absolute temperature. The Arrhenius equation can be linearized by taking the natural log of both sides to produce Equation {2}:

$$\ln\left(\frac{dr}{dt}\right) = \ln(A) - \frac{E}{R} * \left(\frac{1}{T}\right)$$

The Arrhenius coefficients were estimated by finding a linear curve fit between the inverse of the absolute bath temperature and the natural log of the slope of time vs. radius, i.e. dissolution rate, for each bath temperature. This is shown graphically in Figure 9b, which includes a line and equation indicating the linear regression curve fit in which $-7265 = -E/R$ and $8.7853 = \ln(A)$.

To analyze the test data, the Excel @slope() and @intercept() functions were used to directly determine the regression coefficients of the linear fits (as opposed to using the graphical methods shown in Figure 9). In addition to the two-step process outlined above (in which the slopes were determined individually for each solder bath temperature and these slopes were then used to determine the Arrhenius coefficients), a one-step analysis method was also attempted. In this approach, the difference between the starting nominal radius and the radius after immersion was divided by the immersion time to estimate the dissolution rate for each sample. This was then used in a regression analysis to estimate the Arrhenius coefficients. This approach was deemed to be less accurate in analyzing the data due to the uncertainty of the initial wire radii.

TEST RESULTS

Dissolution Rate Measurements

Figure 10 shows a plot of the measured dissolution rates versus the inverse of the absolute temperature of the solder bath with symbols) and curve fits to the Arrhenius equation (with lines) for each material/solder combination evaluated in this study.

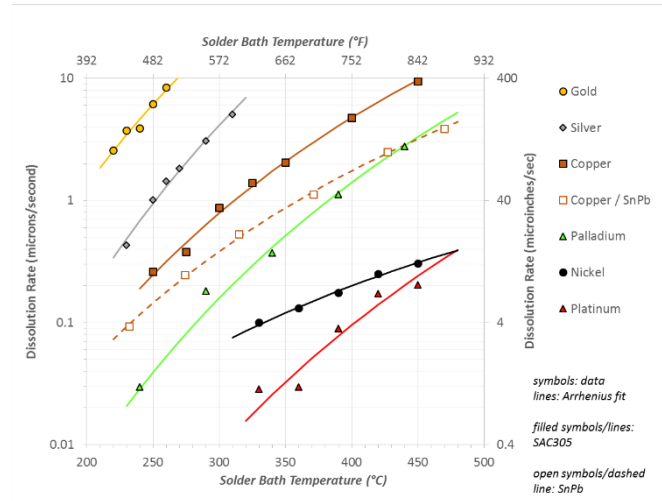


Figure 10: Linearized Dissolution Data vs. Temperature, Current Study {2}

Table 3 shows calculated dissolution characteristics for each material/solder combination. The dissolution values at 250°C and 280°C are reference points that are used, in part, to give a physical sense for the magnitude of the dissolution rate under reflow temperatures. A larger activation energy, E, for the same value indicates lower dissolution for a given temperature but the impact of increased temperature will be larger. The coefficient A has units of dissolution; mathematically, A is the dissolution rate that would occur at an infinite temperature if the solid material and liquid solder remained in their same states. A Monte Carlo simulation approach was used to estimate the uncertainty of the Arrhenius coefficients.

Table 3: Dissolution Characteristics Calculated from Curve Fits of Data

Material / Solder	Dissolution (micron/sec)		E (kJ/mol)	A (mm/s)	R ²
	250°C	@280°C			
Au / SAC	6.12	13.39	62.7	11213	95.9%
Ag / SAC	0.95	2.37	73.4	20140	99.1%
Cu / SAC	0.25	0.51	57.7	144	99.5%
Cu / SnPb	0.14	0.27	48.7	10	99.9%
Pd / SAC	0.039	0.094	69.8	364	98.5%
Ni / SAC	0.032	0.050	35.5	0.11	99.7%
Pt / SAC	0.0021	0.005	74.9	62	95.0%

Figure 11 shows the same data as Figure 10, but in terms of temperature rather than the inverse of the absolute temperature.

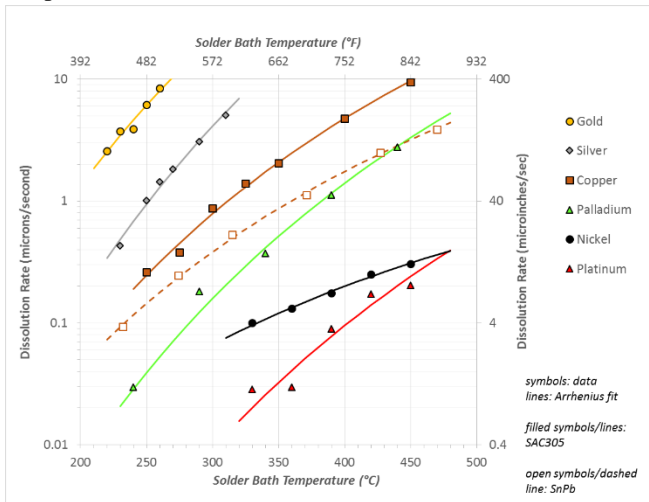


Figure 11: Dissolution Data vs. Temperature, Current Study

The primary observations for the dissolution data:

- The test data are generally well behaved, particularly for the materials with higher dissolution rates, to indicate that the testing included a sufficient number of samples and appropriate duration and temperature combinations. The correlation coefficients (R^2) of 95% and higher indicate that the behavior was well modeled by the Arrhenius equation.
- In general, most of the materials had fairly similar behavior with roughly parallel lines on the linearized plot (Figure 10). Nickel is the exception to this: it showed higher than expected dissolution at lower temperatures but the increase in dissolution rate as temperature increased was less significant.
- The dissolution rate of copper in the SAC305 solder was approximately 0.5-1 order of magnitude higher than with SnPb solder.

Figure 12 combines the measured dissolution rates for SAC305, as determined in this study, to data and curve fits of the Bader data [1] for the dissolution rates of the same materials in SnPb solder. In this plot, solid lines and symbols correspond to SAC305 results while dashed lines/open symbols show results for SnPb.

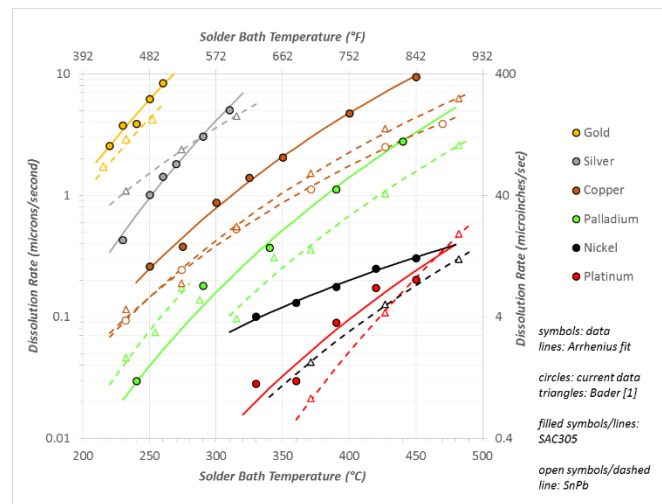


Figure 12: Comparing Dissolution Rates for SAC and SnPb Solders

Significant observations from this plot for the combined data are:

- In most cases, the dissolution rate for a material was higher in SAC305 solder as compared to SnPb. The only exceptions are silver, which exhibited higher dissolution in SnPb for the one test temperature below 250°C in Bader's testing, and palladium at temperatures below ~300°C. Bader had observed that palladium in SnPb exhibited two dissolution rates, with a high dissolution below 274°C that then dropped to a lower rate at temperatures above 315°C.
- Gold and silver, which have the highest dissolution rates, showed similar results for either solder. Copper and palladium dissolution rates were approximately two times higher for SAC305 than with SnPb (except for the anomalous behavior noted by Bader for palladium at temperatures below ~300°C).
- Nickel showed significantly higher dissolution with SAC305 as compared to SnPb. The somewhat unusual behavior for Nickel in SAC305 (a lower slope with temperature) suggests that that test should be re-run to verify that the effects seen with SAC305 are real.
- The results for the only material/solder combination used in both this study and Bader's (Copper with SnPb solder) showed good agreement.

Solder Chemistry Analysis

Prior to testing a set of samples for a given element, the solder pot was filled with virgin SAC305 solder, procured in accordance with IPC-JSTD-006 and a sample of the solder removed from the solder pot for analysis. After testing was completed for each element, a second solder pot sample was removed for analysis so that changes between the "pre-test" and "post-test" conditions of the solder could be determined. Table 4 shows the pre- and post-test solder measurements. The copper, nickel, silver and gold solder pot samples were tested by Qualitek for Optical Emission Spectroscopy

(OES) analysis while the platinum and palladium solder pot samples were evaluated by Indium Corp. with Inductively Coupled Plasma (ICP) analysis. All pre-test solder alloys were shown to be within specifications. Only one of the post-test solder samples exceeded its solder pot contamination limit as defined by IPC-JSTD-001. The solder used in the gold testing exceeded its contamination limit by more than 0.05 %w after the completion of testing. This relatively small amount of excessive contamination in the solder is not likely to have significantly affected the results. It should be noted that there are not specific element contamination control limits for platinum or palladium.

Table 4: Solder Pot Element Test Results

Element Tested	Elemental Wt%		IPC-JSTD-001 Req.	Analysis Method
	Initial	Post		
Cu	0.49	0.68	1.00	ArcSpark OES
Ni	0	0.05	0.05	ArcSpark OES
Ag	2.9	3.18	4.00	ArcSpark OES
Au	0	>0.260	0.20	ArcSpark OES
Pt	<0.001	<0.001	NA	ICP
Pd	<0.001	0.05	NA	ICP

DISCUSSION

A review of the published literature on the dissolution of elements reveals extensive research on gold, silver and copper with less data for nickel, palladium and platinum, with the majority of the work on tin/lead solders and relatively little on lead-free solders. The following sections focus on investigation results versus industry results comparisons for each of the tested elements for both tin/lead and lead-free solders.

Gold

The issue of gold/tin IMC degradation of tin/lead solder joints resulted in significant industry interest and research since the 1960s. Over a period from 1962-1969, Bader [1], Bester [2], Foster [3] and Ebnetter [4] published extensive results on the dissolution rate, formation of the gold/tin IMC and the impact on solder alloy properties. These culminated in Bader's reporting of the dissolution values shown in Figure 13. Berg and Hall [24] further investigated the detrimental effect of gold dissolution on lead/zinc and lead/indium/silver solder alloys to quantify dissolution rates calculated using the same techniques as Bader. Heinzl and Saeger [25] experimentally determined how variations of the gold plating composition and chemistry type influence

the dissolution of gold in pure tin, tin/lead, tin/lead/indium/zinc and tin/lead/cadmium solder alloys. As the implementation of lead-free solder alloys and processes proceeded throughout the industry, the question of the impact of gold dissolution reemerged. Since the SAC305 solder alloy is primarily a pure tin composition, it was believed that the industry knowledge of gold dissolution on tin/lead solder alloys would be applicable. The investigation measured gold dissolution rate in SAC305 solder agrees with Heinzl and Saeger's dissolution rate in pure tin, which validates that assumption. Other results published by Vianco [5] and Puttlitz and Stalter [6] reported the same conclusions, i.e., that tin dominated lead-free solder alloy compositions have the same predictable gold dissolution characteristics that have already been documented in the industry literature. Therefore, new rules/precautions regarding gold dissolution for lead-free solders are probably unnecessary, since the gold dissolution rates for both tin/lead and lead-free solder alloys are both severe enough that any difference between them is inconsequential.

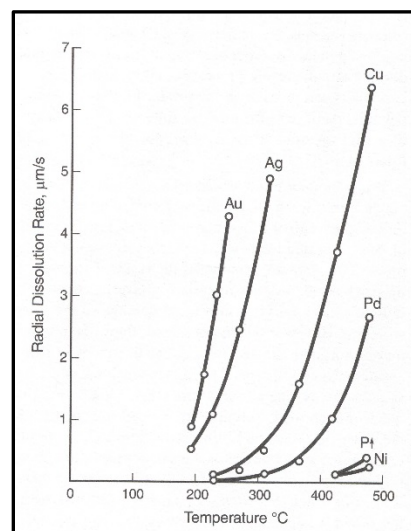


Figure 13: Dissolution Rates of Various Elements in 60Sn40Pb Solder [1]

Silver

The primary industry focus pertaining to the dissolution rate of silver in solder has been on its influence and impact on solder alloy properties. Berg and Hall [24] demonstrated that the dissolution rate of silver increased with increasing tin content of various tin/lead solder alloy compositions. Bulwith and MacKay [26] investigated the dissolution of silver and silver loaded tin/lead/silver solder alloys from the perspective of reducing, or even preventing, silver scavenging of substrate surface finishes. Recent industry-focused investigations of lead-free solder alloys (Puttlitz and Stalter [6]), Anderson [27], Li and Chan [28]) have assessed

how the dissolution and/or diffusion of silver impacts the formation of IMCs, alloy reflow characteristics, solder joint microstructure evolution and solid strength solution strengthening mechanisms. There appears to be minimal industry published results on the basic silver dissolution rate characteristics in lead-free solder alloys; the majority of the published research is on silver diffusion rates. This investigation found that the dissolution of silver in SAC305 solder is slower than gold and faster than copper. Clearly established silver dissolution rates in SAC305 provides benefit to the soldering/manufacturing process industry, which has transitioned to widespread use of immersion silver surface finishes on printed circuit boards.

Copper

The dissolution of copper was recognized as a major concern with the implementation of lead-free soldering technology by the electronic industry. The published industry studies could be placed into two categories: (1) characterizing the impact of copper dissolution on printed circuit assembly integrity; (2) measuring the dissolution rate of copper by lead-free solder alloys for the establishment of process control. Snugovsky et al. [33] conducted extensive thermal cycle testing of various lead-free solder alloys to characterize the interaction of copper dissolution, soldering methodology and solder joint integrity. The results demonstrated process control limits must be strictly adhered to in order to avoid excessive copper dissolution of printed circuit assembly copper structures (i.e. plated through holes, surface mount lands, etc.). Izuta et al. [35] investigated four different lead-free solder alloys including SAC305. Their calculated copper dissolution rate of 1 $\mu\text{m}/\text{second}$ at 260°C of plated through hole coupons in a dynamic solder pot is in reasonable agreement with the 0.35 $\mu\text{m}/\text{second}$ at 260°C copper dissolution rate determined in this study, which used wires in a static solder pot.

Nickel

Nickel plating has been the industry's standard barrier metallization for minimizing solder dissolution of solderable surfaces. Berg and Hall [24] demonstrated that the nickel dissolution rate was consistent for several tin/lead solder alloys when the temperature dependence was taken into account. The current investigation results demonstrated that only platinum had a slower dissolution rate than nickel in the SAC305 solder alloy. The dissolution rates for nickel measured in the investigation are higher than those reported in industry publications (Yang et al. [32], Korhonen et al. [29]). The experimental differences (i.e. metallic foils not wires, pure tin or SAC387 versus SAC305, lower test temperatures, etc.) between those studies and this

investigation account for dissolution rate differences. However, the trend that the nickel dissolution rates are higher with lead-free solder alloys than tin/lead solder alloys was in agreement for all studies.

Palladium

Palladium dissolution does not appear to have been extensively studied. Vianco et al. [30, 36] report data for dissolution in SAC and SnPb solders. Their tests were conducted with strips of material immersed in relatively small quantities of solder. Their reported dissolution rates with SnPb solder were approximately half that found by Bader [1], which were also conducted in a relatively small solder bath but with wire samples instead of strips. The dissolution rate of Pd in SAC solder from the current study was approximately 3x higher than that reported by Vianco et al. [30]. This may be due to a combination of differences between the test approaches used in the two studies, since the current study used wire samples rather than strips and also used a much larger solder bath. Both of these factors appear to increase the dissolution rates measured in testing.

Platinum

There is very little data in the published literature on the dissolution of platinum. Kim and Kim [31] experimentally investigated platinum interactions with three different lead-free solder alloys using metallographic cross-sectional, X-ray diffraction and scanning electron microscopy (SEM) analysis. Platinum dissolution was not included in their study, but they did show that the growth of tin/platinum IMC phases, specifically SnPt₄, was slow, which makes it favorable as a barrier metallization layer. Yang et al. [32] did investigate nickel and platinum dissolution from 250-310°C for a pure tin bath. Their test results showed that platinum dissolution was significantly lower than nickel dissolution which is in agreement with the current investigation results. However, the Yang test results are 5X slower than the current investigation (0.008 $\mu\text{m}/\text{second}$ versus 0.04 $\mu\text{m}/\text{second}$ respectively). This result can be explained by the difference in test methodology as Yang used a solder bath volume of 6 grams (0.013 pounds) versus the current investigation used a solder bath volume of 900 grams (2 pounds). The large solder bath volume resulted in different dissolution interface conditions impacting the dissolution rate. The influence of element concentration gradient on the element dissolution rate has been documented in other studies (Snugovsky et al. [34]).

SUMMARY

Table 5 summarizes data from this study and the literature on elemental diffusion into SnPb and SAC solders. This provides some indication of how test procedures differ in terms of the test sample format and whether dissolution was done in flowing (dynamic) or a fixed (static) bath that is categorized as either small or large to indicate whether the quantity of solder is large enough that its composition would not likely be affected to a significant degree by the material being dissolved into it. For reference, some results with pure tin (Sn) are included with the lead-free (SAC) results.

CONCLUSIONS

The dissolution rates of gold, silver, copper, palladium, nickel and platinum for a SAC305 solder alloy were

determined over a range of temperatures. These values can be used by solder process engineers to create adequate, consistent, solder process temperatures and dwell times that do not impact the integrity of component or printed circuit board surface finishes. The element dissolution rates may also be useful in the avoidance of creating IMC phases such as gold/tin or palladium/tin which would impact solder joint integrity.

ACKNOWLEDGEMENTS

The authors would like to thank and Ken Blazek, Alli Slaughter, Tony Feldmeier, Elena Gladen, Daphne Gates, Henry Ahrenholtz, AOE, for metallurgical cross-sectional tasks.

Table 5: Summary of Reported Dissolution Data for SnPb and SAC305 Solders

Solder	Solid Material	Sample Format	Solder Condition	Dissolution Rate ($\mu\text{m/s}$)		Arrhenius Coefficients		Note	Ref
				@ 250°C	@ 280°C	E (kJ/mol)	A (mm/s)		
SAC	Ag	wire	large static	0.84	2.2	77	4.2e4	a, d	-
		strips	small static	0.14	0.38	79	1.2e4	b	[30]
SAC	Au	wire	large static	6.7	20	87	3.4e6	a, d	-
SAC	Cu	thru hole	dynamic	0.62	1.07	44	14	c	[35]
		substrate	reflow	0.80	-	-	-	b	[29]
		wire	large static	0.29	0.56	53	51	a, d	-
SAC	Ni	wire	large static	0.018	0.033	49	1.5	a, d	-
Sn		strips	small static	0.010	-	-	-	b	[32]
SAC	Pd	wire	large static	0.071	0.14	53	15	a, d	-
		strips	small static	0.017	0.044	77	730	b	[30]
SAC	Pt	wire	large static	0.004	0.009	66	17	a, d	-
Sn		strips	small static	0.003	-	-	-	b	[32]
SnPb	Ag	wire	small static	1.5	2.5	41	17	c	[24]
		substrate	small static	0.63	1.7	77	3.1e4	c	[26]
		wire	small static	1.3	2.1	41	16	a	[1]
SnPb	Au	wire	small static	4.8	10	65	1.3e4	c*	[24]
		wire	small static	4.1	8.5	58	2800	a	[1]
SnPb	Cu	thru hole	dynamic	0.07	0.37	130	7.8e8	c	[35]
		wire	small static	0.13	0.23	45	4.4	c	[24]
		wire	large static	0.16	0.29	48	9.8	a, d	-
		wire	small static	0.23	0.41	44	5.8	a	[1]
SnPb	Ni	wire	small static	0.0025	0.005	57	1.2	c*	[24]
		wire	small static	0.0023	0.0054	70	24	a	[1]
SnPb	Pd	wire	small static	0.16	0.30	50	15	a	[1]
		strips	small static	0.072	0.112	36	0.26	b	[36]
SnPb	Pt	wire	small static	0.0002	0.0007	110	9000	a	[1]

Notes

- a: calculated from the curve fit for the Arrhenius equation of dissolution as a function of time and temperature
- b: used the dissolution rate reported the for maximum exposure time at 250°C and/or 280°C
- c: dissolution rate values obtained from a plot of $\ln(\text{dissolution rate})$ vs. $1/T$
- c*: same approach as c, but the line for $\ln(\text{dr}/\text{dt})$ vs $1/T$ was extrapolated beyond the tested temperature range
- d: refers to results in the current study

REFERENCES

1. W.G. Bader, "Dissolution of Au, Ag, Pd, Pt, Cu and Ni in a Molten Tin-Lead Solder", *Welding Research Supplement*, December 1969, pp. 551S-557S.
2. M. Bester, "Metallurgical Aspects of Soldering Gold and Gold Plating", *InterNEPCON Proceedings*, 1968.
3. F.G. Foster, "Embrittlement of Solder by Gold from Plated Surfaces", *ASTM Special Technical Publications*, No. 319, 1962.
4. S.D. Ebnetter, "The Effect of Gold Plating on Soldered Connections", *NASA Technical Memorandum X-53335*, Oct. 1965.
5. P. Vianco, *Soldering Handbook*, American Welding Society, ISBN 0-87171-618-6, pp. 182-184
6. K. Puttlitz and K. Stalter, "Handbook of Lead-free Solder Technology for Microelectronics Assemblies", Marcel Dekker Inc., ISBN 0-8247-4870-0, pp. 475-480.
7. R.J. Klein Wassink, "Soldering in Electronics", *Electrochemical Publications Limited*, ISBN 0-901150-14-2, pp 107-108.
8. C. Lea, "A Scientific Guide to Surface Mount Technology", *Electrochemical Publications Limited*, ISBN 0-901150-22-3, pp. 107-108.
9. S. Duford, et al., "Microstructural Evolution and Damage Mechanisms in Pb-Free Solder Joints During Extended -40°C to 125°C Thermal Cycles", *IPC Annual Meeting*, 2002, Paper S08-4-1.
10. D. Hillman et al., "The Impact of Reflowing a Pbfree Solder Alloy Using a Tin/Lead Solder Alloy Reflow Profile on Solder Joint Integrity", *CMAP Conf. Proc.*, 2005.
11. R. Wilcoxon, et al., "Solder Joint Integrity Impact of Immersion Silver Surface Finish Thickness for Tin/Lead and Lead-free Solder Processes", *SMTA Int. Conf. on Soldering and Reliability (ICSR)*, May 2008.
12. Texas Instrument Technical Report, "Shelf Life Evaluation of Nickel/Palladium Lead Finish for Integrated Circuits", Report # SZZA002, April 1998.
13. Texas Instrument Technical Report, "Steam Age Evaluation of Nickel/Palladium Lead Finish for Integrated Circuits", Report # SZZA004, April, 1998.
14. P. Vianco, et al., "Assessment of Nickel Palladium Finished Components for Surface Mount Assembly Applications", *SMTAI Conf. Proc.*, Paper 3C7, 1995.
15. R. Pratt, et al., "The Effect of Gold, Silver and Palladium Contamination on the Mechanical Properties of Cu/63Sn-37Pb Solder Joints", *University of Rochester, Sandia Report SAND93-7104*, Sept. 1993.
16. M. Wolverson, "Solder Joint Embrittlement Mechanisms, Solutions and Standards", *IPC APEX EXPO Conference Proceedings*, 2014.
17. P. Tegehall, "Review of the Impact of Intermetallic Layers on the Brittleness of Tin-Lead and Lead-free Solder Joints", *IVF Project Report 06/07*, March 2006.
18. Y. Chen, et al., "Au and Pd embrittlement in space-confined soldering reactions for 3D IC applications, *Advanced Packaging Materials (APM)*", 2013 *IEEE Int. Symp.*, pp. 102 -112.
19. Z. Mei and A. Eslambolchi, "Evaluation of Ni/Pd/Au as an Alternative Metal Finish on PCB), *SMTAI Conf. Proc.*, Paper 3C14, 1998.
20. B. Gumpert et al., "Evaluation of the Use of ENEPIG in Small Solder Joints in Thermal Cycling", *SMTAI Conf. Proc.*, Paper SUB4.2, 2017.
21. M. Wolverson, "Quality, Reliability and Metallurgy of ENEPIG Board Finish and Tin-Lead Solder Joints", *SMTAI Conf. Proc.*, 2011, pp. 960 - 965.
22. L. Garner, et al., "Finding Solutions to the Challenges in Package Interconnect Reliability", *Intel Technical Journal*, Vol. 9, Issue 4, 2005, pp. 297-308.
23. J. Kennedy and D. Hillman, "NASA DoD Phase 2: Sac305 and Sn100c Copper Dissolution Testing", 2013 *SMTA Int. Conf. on Soldering and Reliability Proceedings*, Toronto Canada.
24. H. Berg and E. Hall, "Dissolution Rates and Reliability Effects of Au, Ag, Ni and Cu In Lead Based Solder", *11th Annual Physics Reliability Symp.*, 1973.
25. H. Heinzel and K.E. Saeger, "The Wettability and Dissolution Behavior of Gold in Soft Soldering", *Gold Bulletin*, Vol. 9, Iss. 1, Mar. 1976, pp. 7-11.
26. R.A. Bulwith and C. A. MacKay, "Silver Scavenging Inhibition of Some Silver Loaded Solders", *Welding Research Supplement*, Mar. 1985, pp. 86-90.
27. I.E. Anderson, "Development of Sn-Ag-Cu and Sn-Ag-Cu-X Alloys for Pb-free Electronic Solder Applications", *Lead-free Electronic Solders*, Springer, ISBN 0-387-48431-0, 2007, pp. 55-76.
28. G.Y. Li and Y.C. Chan, "Diffusion and Intermetallic Formation between Pd/Ag metallization and Sn/Pb/Ag Solder in Surface Mount Solder Joints", *Materials Science and Engineering*, B57 (1990), pp. 116-126.
29. T.M. Korhonen et al., "Reactions of Lead-free Solders with CuNi Metallizations", *J. of Electronic Materials*, Vol. 29, No. 10, 2000.
30. P. Vianco et al., "Dissolution and Interface Reactions between Palladium and Tin (Sn)-Based Solders: Part I. 95.5Sn-3.9Ag-0.6Cu Alloy", *Metallurgical and Materials Transactions A*, Vol. 41A, Dec. 2010.
31. T.H. Kim and Y.H. Kim, "Sn-Ag-Cu and Sn-Cu Solders: Interfacial Reactions with Platinum", *J. of Materials*, June, 2004.
32. S.C. Yang et al., "Interfacial Reaction and Wetting Behavior between Pt and Molten Solder" *J. of Electronic Materials*, Vol. 38, No. 1, 2009.
33. P. Snugovsky et al., "Microstructure and Reliability Comparison of Different Pb-free Alloys Used for Wave Soldering and Rework", *J. of Electronic Materials*, Vol. 38, No. 12, 2009.
34. L. Snugovsky et al., "Experiments on Interaction of Liquid Tin with Solid Copper", *J. of Materials Science and Technology*, July 2003, Vol. 19.
35. G. Izuta, et al., "Dissolution of Copper on Sn-Ag-Cu System Lead-free Solder", *Soldering & Surface Mount Technology*, Vol. 19, No. 2, 2007.
36. P. Vianco et al., "Dissolution and Interface Reactions between Palladium and Tin (Sn)-Based Solders: Part II. 63Sn-37Pb Alloy", *Metallurgical and Materials Transactions A*, Vol. 41A, Dec. 2010, pp. 3053-3064.